MODEL INTER-COMPARISON AND EVALUATION OF DUST FORECASTS

SDS-WAS-2020-001

E. Terradellas[1], S. Basart[2], E. Werner[1] and F. Benincasa[2]

[1]*Agencia Estatal de Meteorología (AEMET), Barcelona, Spain*

[2]*Supercomputing Center (BSC), Barcelona, Spain*

25 May 2022

TECHNICAL REPORT

Series: Sand and Dust Storm Warning Advisory and Assessment System (SDS-WAS) Regional Center for Northern Africa-Middle East-Europe (NAMEE) Technical Report

A full list of SDS-WAS NAMEE Regional Center Publications can be found on our website under:

http://sds-was.aemet.es/materials/technical-reports

Sand and Dust Storm Warning Advisory and Assessment System (SDS-WAS) Regional Center for Northern Africa-Middle East-Europe (NAMEE)

C/Jordi Girona, 29 | 08034 Barcelona (Spain)

Summary

This document describes the dust forecast inter-comparison and model evaluation available in the Regional Center for Northern Africa, Middle East and Europe (hereafter RC NAMEE or RC) of the World Meteorological Organization (WMO) Sand and Dust Storm Warning Advisory and Assessment System (SDS-WAS).

Please, be aware that the document is being revised regularly with the incorporation of the new models and observations. **Last revision is done on 25th May 2022.**

Contents

1. Introduction

The **Sand and Dust Storm Warning Advisory and Assessment System (SDS-WAS)** is a project of the World Meteorological Organization (WMO) with the mission to enhance the ability of countries to deliver timely and quality sand and dust storm forecasts, observations, information and knowledge to end users. The Regional Center for Northern Africa, Middle East and Europe (hereafter RC NAMEE or RC), hosted by the Spanish State Meteorological Agency (AEMET) and the Barcelona Supercomputing Center (BSC), supports a network of research and operational partners implementing the objectives of the SDS-WAS program in the region.

The exchange of forecast model products is recognized as a core part of the WMO SDS- WAS activities, as a key contribution to the RC NAMEE and as a basis for the model inter-comparison and evaluation. The SDS-WAS model inter-comparison and evaluation will make use of a wide range of available datasets describing different aspects of the atmospheric dust cycle. The results of this experiment are expected to **improve the dust parameterization in the individual models and ultimately improve dust forecasts**.

There was a preliminary list of modelling systems providing daily operational or pre-operational dust forecast products. However, it was quite difficult to gather homogeneous products from the different partners and was decided (3rd. and 4th. SDS-WAS RC phone meetings) to start concentration of five models (BSC-DREAM8b, MACC, CHIMERE, LMDzT-INCA, and DREAM-NMME-MACC). Other models have been incorporated throughout the following years.

2. Forecast products

2.1. General features

The **geographical area of interest** is bounded by the following coordinates: latitude 25°W to 60°E and longitude 0° to 65°N (see Figure 1). It is called the **Reference Area (RA)** and is intended to cover the main source areas in Northern Africa and Middle East, as well as the main transport routes and deposition zones from the equator to the tip of the Scandinavian Peninsula.

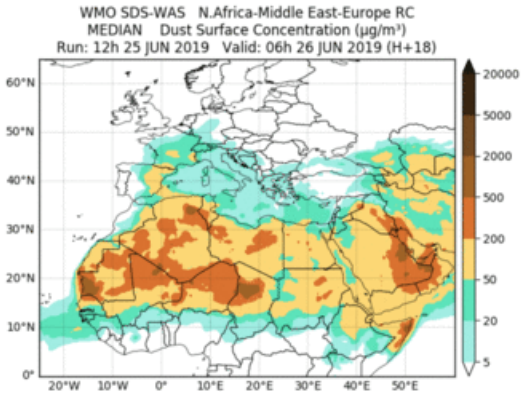

***Figure 1**: The SDS-WAS Multi-model Median surface concentration dust forecast for 26th June 2019 at 6UTC. The domain shown is the Reference Area (RA) is the considered by the RC NAMEE.*

The **variables** to be provided and their corresponding units are:

- Dust aerosol concentration at the surface (SCONC_DUST), instantaneous (kg·m-3)
- Dust optical depth at 550 nm (AOD550_DUST), instantaneous (adimensional)

The action will consider forecasts with lead times up to 72 h, based on 00 UTC or 12 UTC runs. The output frequency is of 3 hours. The products shall be daily available, ready for download by the RC team.

2.2. Forecasts models

In Table 1, there is listed the models have provided daily dust forecasts to the RC NAMEE.

Table 1. *Overview of the the models that have been contributed to the SDS-WAS multi-model intercomparison since the starting of the RC NAMEE. In red colour, those models that at present, are not providing dust forecasts to the RC NAMEE.*

Model	Institution	Domain	PI or contact
BSC-DREAM8b	BSC	Regional	Sara Basart <sara.basart@bsc.es>
CHIMERE	LMD	Regional	Laurent Menut
LMDzT-INCA	LSCE	Global	Michael Schulz
CAMS-ECMWF	ECMWF	Global	Angela Benedetti <Angela.Benedetti@ecmwf.int>
DREAM-NMME-MACC	SEEVCCC	Regional	Goran Pejanovic <goran.pejanovic@hidmet.gov.rs>
NMMB-MONARCH	BSC	Regional	Sara Basart <sara.basart@bsc.es>
MetUM	MetOffice	Global	Melissa Brooks <melissa.brooks@metoffice.gov.uk>
GEOS-5	NASA	Global	Arlindo da Silva <arlindo.dasilva@nasa.gov>
NGAC	NCEP	Global	Jun Wang <Jun.Wang@noaa.gov>
EMA REG CM4	EMA	Regional	Ashraf Zakey <ashraf.zakey@yahoo.com>
DREAMABOL	CNR-ISAC	Regional	Alberto Maurizi <a.maurizi@isac.cnr.it>
WRF-CHEM	NOA	Regional	Emmanouil Flaounas <flaounas@noa.gr>
SILAM	FMI	Global	Mikhail Sofiev <mikhail.sofiev@fmi.fi>
WRF-Chem	NOA	Regional	Vassiliki Kotroni <kotroni@meteo.noa.gr>
LOTOS-EUROS	TNO	Regional	Astrid Manders-Groot <astrid.manders@tno.nl>
ICON-ART	DWD/KIT	Regional	Vanessa Bachmann <Vanessa.Bachmann@dwd.de>
DREAM8-NMME-MSG	IAASARS/NOA	Regional	Stavros Solomos <stavros@noa.gr>
ALADIN-Dust	MetOffice of ALGERIA	Regional	Abdenour AMBAR <ambar.abdenour@gmail.com>
WRF-NEMO-CAMx	Aristotle University of Thessaloniki	Regional	Serafim Kontos <serkontos@gmail.com>
ZAMG-WRF-CHEM	ZAMG	Regional	Barbara Scherllin-Pirscher \barbara.scherllin-

			pirscher@zamg.ac.at> Marcus Hirtl <marcus.hirtl@zamg.ac.at>
MOCAGE	MétéoFrance	Global	Vincent Guidard <vincent.guidard@meteo.fr>

Each modelling group has provided a short report on the main features of its model. The model characteristics are summarized in Table 2 and described in more detail in **Appendix A**.

***Table 2**. Model description. This table include the main features of the model configuration used by each modelling group.*

Model	**BSC-DREAM8b**	**CHIMERE**	**LMDzT-INCA**	**CAMS**
Institution	BSC	LMD	LSCE	ECMWF
Meteorological driver	Eta/NCEP	MM5	LMDzT	ECMWF
Regional or global coverage	Regional	Regional	Global	Global
Meteorological initial fields	NCEP/GFS	NCEP/GFS	ECMWF/IFS	ECMWF/IFS
Emission scheme	Uplifting (Shao et al., 1993; Janjic et al., 1994; Ginoux et al., 2001)	Saltation and sandblasting (Marticorena and Bergametti, 1995; Alfaro and Gomes, 2001; Menut et al., 2005)	Uplifting (Schulz et al., 1998; Schulz, 2007; Guelle et al., 2000)	Uplifting (Ginoux et al., 2001; Morcrette et al., 2008, 2009)
Horizontal resolution	1/3° x 1/3°	1° x 1°	3.75°x2.85°	8-10 km approx. (O1280)
Vertical resolution	24 Eta-layers	30 sygma-layers	19 sygma-hybrid-layers	137 sygma-layers
Height first layer	86 m (above sea level)	40 m (above the surface)	120 m (above surface)	10 m (above the surface)
Radiation interactions	Yes	No	No	No
Transport size bins	8 bins (0.1-10μm)	9 bins (0.039-20μm)	1-log normal mode, mass and number (width 2, MMD varying 1.5-2.5 μm)	3 bins (0.03-20μm)
Data assimilation	No	No	No	Yes AOD550/MODIS

Table 2. Continuation.

Model	**DREAM8-NMME-CAMS**	**NMMB-MONARCH**	**MetUM**	**GEOS-5**
Institution	SEEVCCC	BSC	Met office	NASA
Meteorological driver	NMME	NMMB/NCEP	MetUM	GEOS-5
Regional or global coverage	Regional	Regional	Global	Global
Meteorological initial fields	ECMWF/IFS	NCEP/GFS	MetUM	GEOS-5 Analysis
Emission scheme	Uplifting (Shao et al., 1993; Janjic et al., 1994)	Saltation and sandblasting (Janjic qt al., 1994; Marticorena and Bergametti, 1995)	Woodford (2001, 2011)	Based on Ginoux (2001)
Horizontal resolution	1/3º x 1/3º	1/3º x 1/3º	0.3516º x 0.2344º	0.25º x 0.3125º
Vertical resolution	24 Eta- layers	24 sygma-hybrid-layers	70 levels. Charney-Phillips grid	72 layers. Top: 0.01 hPa
Height first layer	96 m (above sea level)	108 m (above surface)	20 m	
Radiation interactions	No	Yes	Yes	Direct effects fully included
Transport size bins	8 bins (0.1-10μm)	8 bins (0.1- 10μm)	2 (0.1-10 μm)	5 bins centered at (0.73μm,1.4 μm,2.4μm,4.5 μm,8.0 μm)
Data assimilation	Yes (ECMWF dust-analysis)	No	Yes (MODIS/Aqua)	Yes (MODIS)

Table 2. Continuation.

Model	**NGAC**	**EMA RegCM4**	**DREAMABOL**	**WRF-CHEM**
Institution	NCEP	EMA	CNR-ISAC	NOA
Meteorological driver	NEMS GFS	RegCM4	BOLAM	WRF
Regional or global coverage	Global	Regional	Regional	Regional
Meteorological initial fields	NCEP/GDAS	NCEP/GFS	NCEP/GFS	NCEP/GFS
Emission scheme	Dust uplifting followin g Ginoux (2001)	Saltation and sandblasting (A.S. Zakey, 2006; Marticorena and Bergametti, 1995; Alfaro and Gomes, 2001)	Uplifting (Tegen et al., 1994)	Gocart scheme by Ginoux et al. (2001)
Horizontal resolution	T126 (~ 1°)	45 km x 45 km	0.4° x 0.4°	0.19° x 0.22°
Vertical resolution	64 sigma-pressure hybrid layers, Top at 0.2 hPa	18 sygma-layers	50 sigma-hybrid levels	30 sigma levels
Height first layer	20 m	50 m	27 m above surface level	
Radiation interactions	Yes (not activated)	Yes (both short and long waves)	Not active	No
Transport size bins	5 bins centered at (0.73,1.4, 2.4, 4.5, 8.0 μm)	4 bins(0.01:1,-1:2.5 - 2.5:5 - 5:20)	8 bins (0.1-10μm)	5 bins (0.5, 1.4, 2.4, 4.5, 8μm)
Data assimilation	No	No	No	No

Table 2. Continuation.

Model	**SILAM**	**LOTOS-EUROS**	**ICON-ART**	**DREAM8-NMME-MSG**
Institution	FMI	TNO	DWD + KIT	IAASARS/NOA
Meteorological driver	ECMWF	ECMWF	DWD	NCEP/NMME
Regional or global coverage	Global	Regional	Regional	Regional
Meteorological initial fields	ECMWF	ECMWF	ICON-ART Global with nested domain over NAMEE	NCEP/GFS
Emission scheme	Sandblasting following Marticorena & Bergametti, 1995, updated with Zender, 2003, Weinzierl, 2007, Prigent et al., 2007	Marticorena& Bergametti 1995. Dust uplifting following Shao et al. (2001).	Saltation and threshold friction velocity for dust emission flux (Rieger et al., 2017; Vogel et al., 2006; White, 1979; Shao and Lu, 2000; Alfaro and Gomes, 2001).	Dust uplifting following Shao et al. (1993) I ncluding the viscous sublayer approach (Janjic, 1994)
Horizontal resolution	0.5° x 0.5°	1/2° x 1/4°	40 km global + 20 km two-way nest	1/5°×1/5°
Vertical resolution	28 hybrid sigma-pressure levels	4 dynamical layers + surface layer	90 (global) and 60 (nest) Smooth Level Vertical SLEVE coordinate (Leuenberger 2010)	28 hybrid layers
Height first layer	~50m above surface level	25 m above surface level	10 m above the surface	50 m above sea level (approx.)
Radiation interactions	No	No	Yes	No
Transport size bins	5 bins (0.1-1, 1-2.5, 2.5-10, 10-30 μm)	5 bins (0.1-10μm)	3-log normal modes for mass and number concentration	8 bins (0.1-10μm)
Data assimilation	No	No	No	Yes (MSG-SEVIRI over land)

Table 2. Continuation.

Model	**ALADIN-Dust**	**WRF-NEMO-CAMx**	**ZAMG-WRF-CHEM**	**MOCAGE**
Institution	ONM-Algeria	Aristotle University of Thessaloniki	ZAMG	METEO FRANCE
Meteorological driver	ALADIN	WRF	WRF	ARPEGE
Regional or global coverage	Regional	Regional	Regional	Global
Meteorological initial fields	ARPEGE	NCEP/GFS	IFS forecasts	ARPEGE
Emission scheme	Dust Entrainment And Deposition (DEAD) model (Zender et al., 2003	Horizontal mass flux of Owen (1964), threshold friction velocity from Marticorena and Bergametti (1995), drag partition of Raupach et al. (1993) as in Darmenova et al. (2009) and sandblasting efficiency of Alfaro and Gomes (2001).	AFWA dust emission scheme for the GOCART aerosol model (LeGrand et al. 2019), tuning factors for friction velocity, soil moisture, preferential dust source term, and bulk vertical dust emission flux activated	Marticorena and Bergametti (1995)
Horizontal resolution	25km x 25km	18km x 18km	0.2°x 0.2°	1° x 1°
Vertical resolution	70 σ-layers	18 layers up to 100hPa	47 vertical eta levels, model top at 50 hPa	47 levels (global)
Height first layer	65m above the surface (approx.)	30 m above the surface (approx.)	~25 m above the surface	~20 m (above the surface)
Radiation interactions	Yes	No	Not activated	No
Transport size bins	3 bins (0.078-5μm)	2 bins (0.036-2.5 μm and 2.5-10 μm in diameter)	5 dust bins, log-normal size distribution; effective radii of 0.73 μm, 1.4 μm, 2.4 μm, 4.5 μm, and 8 μm	6 bins (2.0E-3, 0.01, 0.1, 1, 2.5, 10, 50 microns)
Data assimilation	No	No	No	Yes, MODIS and VIIRS

2.2.1. Numerical data format

The format for data exchange is NetCDF, with one file per model run. The format has been

developed and mantained at Unidata, which is part of the U. S. University Corporation for Atmospheric Research (UCAR). It allows data compression while preserving characteristics of numerical fields that have a very large dynamical range.

The exchanged files meet the following standards:

- One netcdf file with the daily run (at 00 or 12 UTC). The filename is YYYYMMDDHH_3H_MODELNAME.nc where YYYYMMDDHH is date and time of the model run and MODELNAME is a name selected by the modeler
- Any regular lat-lon domain
- Two variables: dust surface concentration (SCONC_DUST) and dust optical depth at 550 nm (OD550_DUST)
- Forecast time from 0 to 72 hours every 3 hours

The numerical dust forecast outputs are accessible through the SDS-WAS RC website.

3. SDS-WAS Multi-model products

The SDS-WAS Multi-model products are generated from the different prediction models. Two products describing centrality (**median** and **mean**) and two products describing spread (standard deviation and range of variation) of the multi-model ensemble are daily computed (Figure 2). In order to generate them, the model outputs are bi-linearly interpolated to a common grid mesh of 0.5º x 0.5º. Median values ranging from the initial day at 15:00 UTC to the following day at 12:00 UTC are also included in the model intercomparison and the model evaluation.

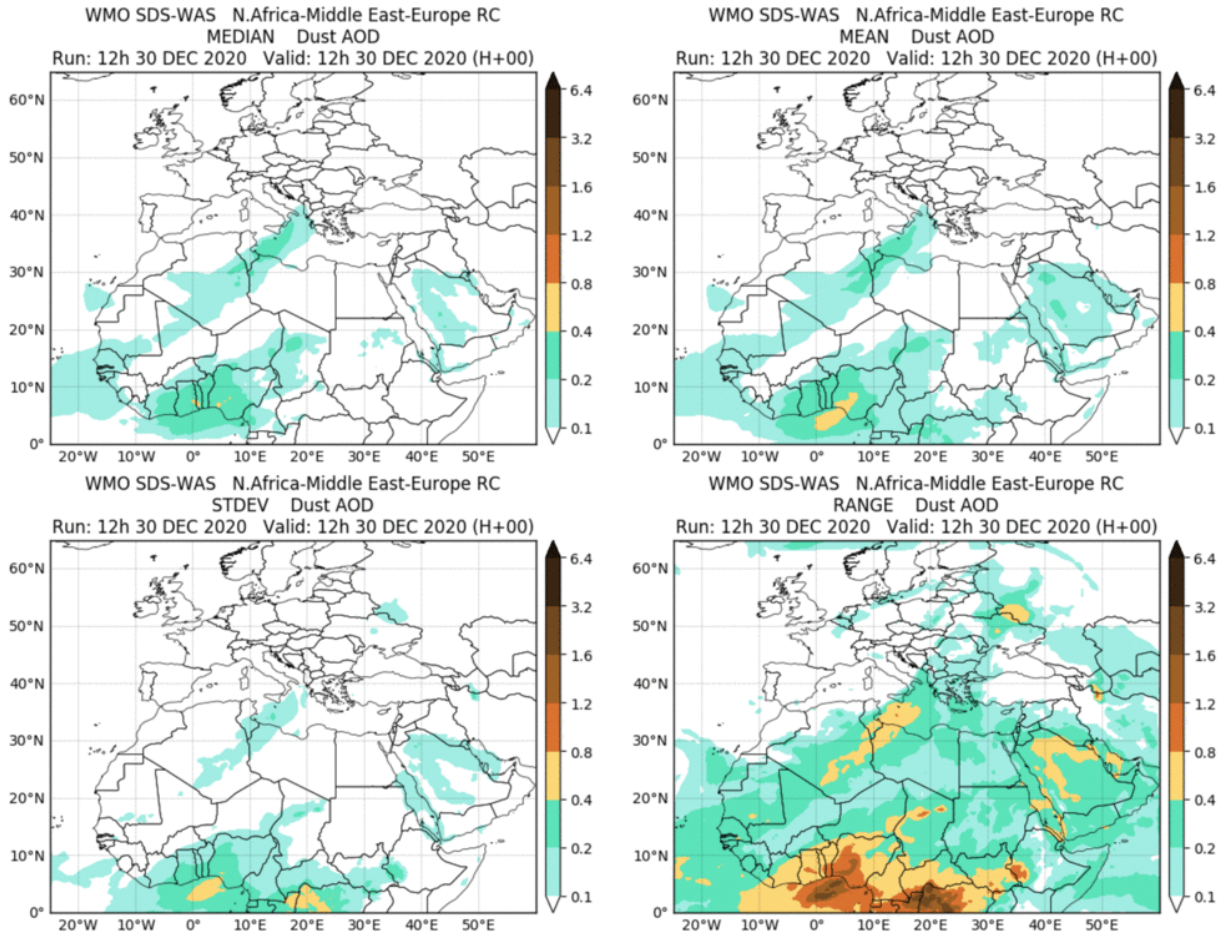

***Figure 2**: The SDS-WAS ensemble dust optical depth (DOD) forecast for 30th December 2020 at 12UTC.*

4. Forecast visualisation

The values of dust surface concentration and dust optical depth provided by each model are daily plotted side-by-side for the RA using a common color palette (see Table 3 and Figure 3). The palette has been built by combining brownish and greenish colours. The brownish tones highlight the areas with the highest contents of mineral dust whereas the greenish tones allow emphasizing the thresholds set by European Union directives on air quality. An extra color (gray) has been defined for missing data (eventually non-available products or areas outside the integration bounds of limited-area models).

***Table 3**: SDS-WAS colour palette to display dust forecasts.*

DOD	0 to 0.1	0.1 to 0.2	0.2 to 0.4	0.4 to 0.8	0.8 to 1.2	1.2 to 1.6	1.6 to 3.2	3.2 to 6.4	> 6.4
Conc, (ug/m3)	0 to 5	5 to 20	20 to 50	50 to 200	200 to 500	500 to 2000	2000 to 5000	5000 to 20000	> 20000
Colour									
RGB	255,255,255	161,237,227	92,227,186	252,215,117	218,114,48	158,98,38	113,73,33	57,37,17	29,19,9

The plots are routinely generated and made available at the end of each day using the results of the simulations starting the same day either at 00 or at 12 UTC. In this manner, forecasts released by the models are available for a common period of up to 48 hours, thus making the product a powerful tool to issue short-term predictions and early warning notices. The latest forecasts, as well as historical plots, are available at: http://sds-was.aemet.es/forecast-products/compared-dust-forecasts

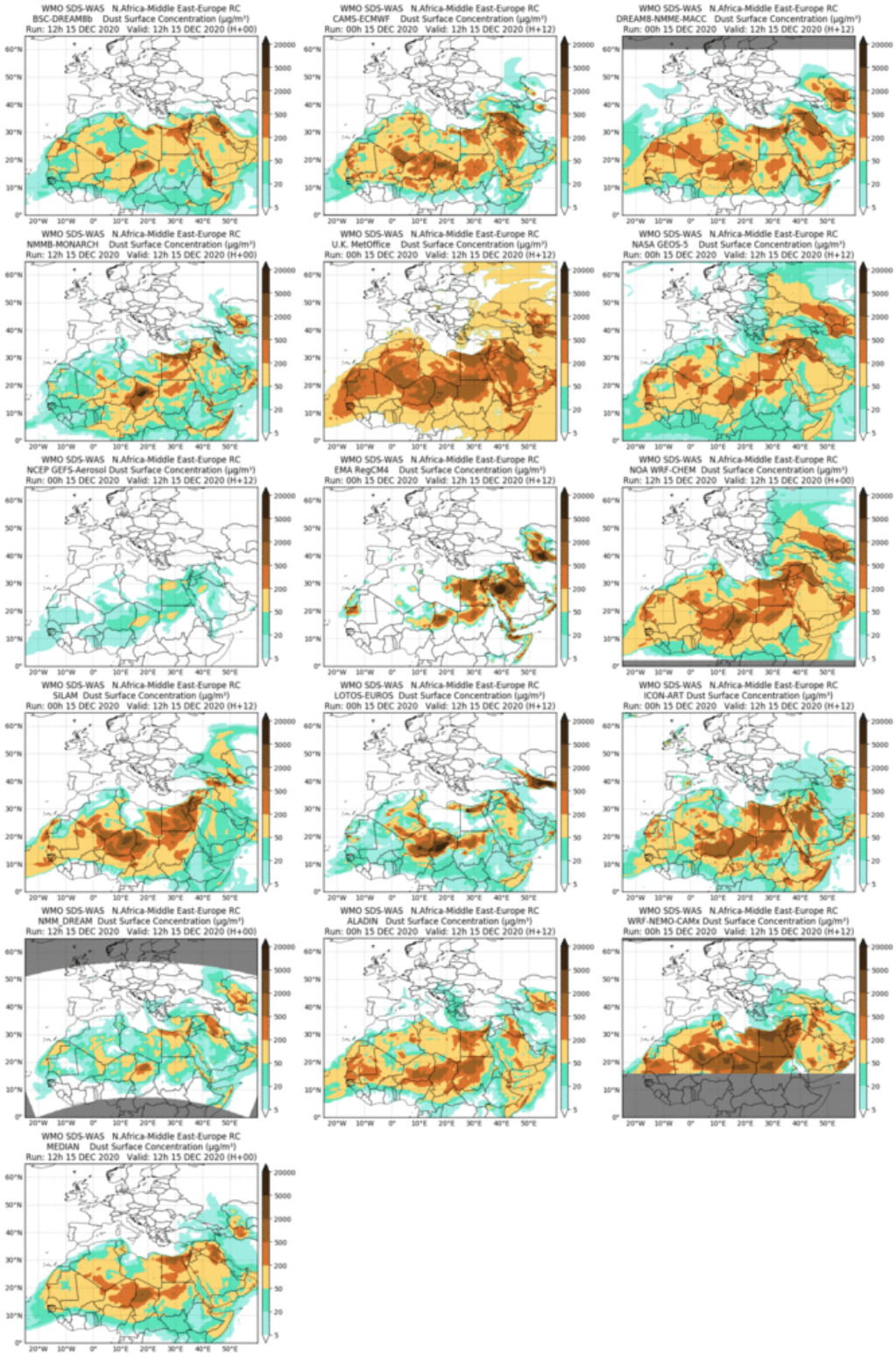

***Figure 3**: SDS-WAS Multi-model comparison of surface concentration dust forecasts for 30th December 2020 at 12UTC.*

5. Model evaluation

5.1. Observations

The first problem for the evaluation of dust models is the scarcity of routine observations intended for dust monitoring. By the moment, aerosol optical depth (AOD) from sun-photometric measurements and satellite aerosol products are used in the present exercise.

Direct-sun photometric measurements provide retrieval of column-integrated aerosol properties. The Aerosol Robotic Network (AERONET) is a set of stations that provides aerosol retrievals in near-real-time (Holben et al., 1998; Dubovik and King, 2000). A major shortcoming of these measurements is their unavailability under cloudy skies and during nighttime. However, they are by far the most commonly used in dust model evaluation.

Satellite products have the advantage of a large spatial coverage and that measurements are regular and rapidly available. However, they are highly integrated over the column and over all aerosol components. Therefore, applications involving a particular aerosol type (like dust) are usually limited to seasons and regions, when or where that type dominates the aerosol composition (Basart et al, 2012). For the SDS-WAS model evaluation, it is considered the aerosol products from NASA/MODIS. There are different algorithms to retrieve aerosol optical depth (AOD) from the MODIS spectrometer travelling on board the Terra and Aqua satellites.

The U. S. Naval Research Laboratory (NRL) and the University of North Dakota (UND) developed a value-added NRT AOD product specifically designed for quantitative applications including data assimilation and model validation. It is generated every six hours, and time-stamped 00:00, 06:00, 12:00, and 18:00 UTC, including MODIS observations from +/-3 hours from the timestamp and near-real-time available through the NASA's EOSDIS system. It gives values of the total AOD without any information for partitioning between dust and other aerosol species.

Because of the difficulty in separating the signals of aerosols from those of highly reflective surfaces, aerosol retrievals over bright surfaces, such as deserts, have been limited. The MODIS Deep Blue aerosol retrieval algorithm uses the blue channels; where the surface contribution is relatively low, to retrieve aerosol properties over such regions (Hsu et al., 2004; 2006). The mean value of the MODIS Deep Blue aerosol optical depth retrieval is used for the evaluation whereas the mean value of the Angstrom exponent 0.412-0.47 μm is used to identify those areas where mineral dust is the dominant source of atmospheric aerosol. The Deep Blue retrievals are included in the NASA's Level-3 MODIS Atmosphere Daily Global Product. All statistics are sorted into 1° × 1° cells on an equal-angle global grid.

Since November 2017, the NASA's MODIS aerosol products considered correspond to Collection 6.1.

5.2. Evaluation metrics

The common metrics that are used to quantify the mean departure between modelled (c_i) and observed (o_i) quantities are the mean bias error (BE), the root mean square error (RMSE), the correlation coefficient (r) and the fractional gross error (FGE). They are presented in Table 4, where n denotes the number of data.

Table 4. Summary of the statistical metrics that will be used in the model evaluation.

Statistic Parameter	Formula	Range	Perfect score	Description
Mean Bias Error (BE)	$BE = \frac{1}{n}\sum_{i=1}^{n}(c_i - o_i)$	∞ to +∞	0	It captures the average deviations between two datasets. It has the units of the variable. Values near 0 are the best, negative values indicate underestimation and positive values indicate overestimation.
Root Mean Square Error (RMSE)	$RMSE = \sqrt{\frac{1}{n}\sum_{i=1}^{n}(c_i - o_i)^2}$	0 to +∞	0	It combines the spread of individual errors. It is strongly dominated by the largest values, due to the squaring operation. Especially in cases where prominent outliers occur, the usefulness of RMSE is questionable and the interpretation becomes more difficult.
Correlation coefficient (r)	$r = \frac{\sum_{i=1}^{n}(c_i - \bar{c})\cdot(o_i - \bar{o})}{\sqrt{\sum_{i=1}^{n}(c_i - \bar{c})^2}\cdot\sqrt{\sum_{i=1}^{N}(o_i - \bar{o})^2}}$	-1 to 1	1	It indicates the extent to which patterns in the model match those in the observations.
Fractional Gross Error (FGE)	$FGE = \frac{2}{n}\sum_{i=1}^{n}\left\|\frac{c_i - o_i}{c_i + o_i}\right\|$	0 to 2	0	It is a measure of model error, ranging between 0 and 2 and behaves symmetrically with respect to under- and overestimation, without over emphasizing outliers.

5.3. Evaluation methods

5.3.1. Comparison with AERONET

The dust optical depth (DOD) forecast are compared with the total aerosol optical depth (AOD) provided by the AERONET network for a selection of dust-prone stations located in Northern Africa, Middle East and Southern Europe that are listed in **Appendix B**. Since January 2017, **Version 3 Level 1.5 of AERONET products** are used for the near- real-time (NRT) evaluation. AERONET Level 1.5 data are automatically cloud screened but may not have final calibration applied. Before that date, Version 2 products had been used. In Basart et al. (2017) show the comparison between AERONET Version 2 and 3.

Since AERONET sun photometers do not yield AOD at 550 nm (AOD550), this variable is calculated from AOD at 440, 675 and 870 nm (AOD440, AOD675, AOD870) and the Ångström exponent 440-870 (AE440_870) using the Ångström law:

$$AOD\,550 = \frac{1}{3}\left(AOD\,440\left(\frac{440}{550}\right)^{AE\,440_{870}} + AOD\,675\left(\frac{675}{550}\right)^{AE\,440_{870}} + AOD\,870\left(\frac{870}{550}\right)^{AE\,440_{870}} \right)$$

To minimize the sources of error, it is intended to restrict the comparison to situations in which mineral dust is the dominant aerosol type. Threshold discrimination is made by discarding observations with an Ångström exponent 440-870 higher than 0.6 (Pérez et al., 2006b).

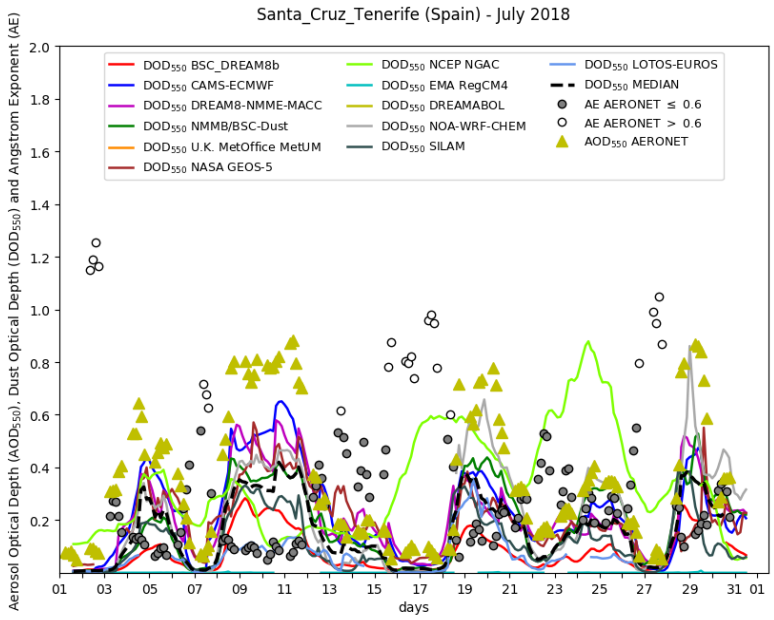

***Figure 4**: SDS-WAS Multi-model comparison of dust optical depth forecasts for July 2018.*

Since January 2017, coinciding with introduction of Version 3 products, AERONET observations are interpolated within 3-hour windows centered at multiple-of-3 hours. Before that date, the closest-in-time retrieval was considered. This resulting dataset is used for the NRT evaluation (see Figure 4) in which all the dust forecast are compare in the selected AERONET sites and for the calculation of quantitative scores.

To get the performance of the different models participating in this SDS-WAS Multi-model intercomparison, a system to evaluate the performance of the different models has been set. The system yields, on a monthly, seasonal and annual basis, evaluation scores computed from the comparison of the simulated dust optical depth (DOD) and the dust-filtered direct-sun AOD observations from AERONET.

The evaluation system is applied to instantaneous forecast values of DOD ranging from the initial day (D) at 15:00 UTC to the following day (D+1) at 12:00 UTC. It means that the lead times of forecasts to be evaluated range from 15 to 36 hours for model runs starting at 00 UTC, but from 3 to 24 hours for model runs starting at 12 UTC.

The scores of each model and median multi-model are computed for each AERONET site, for the 3 sub-regions (Sahel/Sahara, Middle East and Mediterranean; see **Appendix B**) as well as globally considering all sites. It should be noted that scores for individual sites can be little significant for being calculated from a small number of data.

Although observations with an Ångström exponent 440-870 higher than 0.6 are discarded in order to restrict the evaluation to situations in which mineral dust is the dominant aerosol type, other particles are always present (anthropogenic aerosol, products from biomass burning, etc.). Therefore, negative bias can be expected.

5.3.2. Comparison with MODIS

The model evaluation of Saharan dust transport onto the Atlantic uses the MODIS value-added NRT AOD product described in Section 5.1. Since this aerosol product does not provide any information for partitioning between dust and other aerosol species, the evaluation is restricted to an oceanic area, where it is known that mineral dust is by far the main source of atmospheric aerosol. The area, extending between 15º and 30º N and between 18º and 25º W, is the way of Saharan dust out to the Atlantic. As it was the case in the evaluation with AERONET data, although mineral dust is the dominant aerosol in the region, other particles are likely present and, therefore, a negative bias is expected.

- The forecasts of DOD at 12:00 and 18:00 of D+1 are compared with the corresponding MODIS-derived values of AOD. The granules of 00:00 and 06:00 are not used, because neither Terra nor Aqua fly over the area of interest at that times. Model forecasts are bi-linearly interpolated to a 0.5º x 0.5º mesh grid in order to match the spatial resolution of the MODIS retrievals.

- The scores of each model are computed on a monthly, seasonal and annual basis. In the monthly evaluations, model runs between the first and the last day of the month are compared with MODIS retrievals between the second day of the month and the first day of the following month. Only those models that do not use MODIS-derived data in the data assimilation process are considered.

The model evaluation with MODIS Deep Blue retrievals is based on the Aqua/MODIS Deep Blue products.

- The Aqua satellite turns in a sun-synchronous orbit. Its overpass time is around 12:00 local time in its ascending (daytime) mode. The forecasts of dust optical depth (DOD) at 12:00 of D+1 are compared with the corresponding MODIS-derived values of AOD. The maximum lag between observation and prediction is of 3-4 hours.

- It is intended to restrict the comparison to situations in which mineral dust is the dominant aerosol type. Threshold discrimination is made by discarding observations with a MODIS-retrieved Ångström exponent 412-490nm higher than 1.0. However, besides dust, there might be other aerosol types (anthropogenic source, biomass fire, etc.) and, therefore, a negative bias can be expected in the scores.

- Model forecasts are bi-linearly interpolated to a 1º x 1º mesh grid in order to match the spatial resolution of the MODIS deep blue retrievals. Only those models that are not using MODIS-derived AOD in the data assimilation process are considered in this model evaluation.

- The scores of each model are computed on a monthly, seasonal and annual basis. In the monthly evaluations, model runs between the first and the last day of the

month are compared with MODIS retrievals between the second day of the month and the first day of the following month.

6. References

Alfaro, S. C. and Gomes, L. (2001): Modeling mineral aerosol production by wind erosion: emission intensities and aerosol size distributions in source areas, J. Geophys. Res.-Atmos., 106, 18075–18084, https://doi.org/10.1029/2000JD900339.

Alfaro, S. C., and Gomes, L. (2001): Modeling mineral aerosol production by wind erosion: Emission intensities and aerosol size distributions in source areas, Journal of Geophysical Research, 106, 18075-18018, 18084.

Balkanski, Y., M. Schulz, T. Claquin and S. Guibert (2006), Reevaluation of mineral aerosol radiative forcings suggests a better agreement with satellite and AERONET data, Atmos. Chem. Phys., 7, 81-95, doi:10.5194/acp-7-81-2007.

Basart, S. (2017): Forecast Evaluation: AERONET vs. SDS-WAS multimodel forecast, WMO SDS-WAS, Barcelona, 7 pp., SDS-WAS-2017-001.

Basart, S., C. Pérez, S. Nickovic, E. Cuevas, and J. M. Baldasano (2012), Development and evaluation of the BSC-DREAM8b dust regional model over Northern Africa, the Mediterranean and the Middle East, Tellus B, 64, 18539.

Bechtold, P., E. Bazile, F. Guichard, P. Mascart and E. Richard, A mass flux convection scheme for regional and global models, Quart. J. Roy. Meteor. Soc., 127, 869-886, 2001.

Benedetti, A., J.-J. Morcrette, O. Boucher, A. Dethof, R. J. Engelen, M. Fisher, H. Flentjes, N. Huneeus, L. Jones, J. W. Kaiser, S. Kinne, A. Mangold, M. Razinger, A.

Bessagnet, B., Menut, L., Aymoz, G., Chepfer, H. and Vautard, R. (2008): Modelling dust emissions and transport within Europe: the Ukraine March 2007 event, J. Geophys. Res., 113, D15202, doi:10.1029/2007JD009541.

Colarco, P.R., A. da Silva, M. Chin and T. Diehl (2010), Online simulations of global aerosol distributions in the NASA GEOS-4 model and comparisons to satellite and ground-based aerosol optical depth, J. Geophys. Res. doi:10.1029/2009JD012820.

DARMENOVA, K., SOKOLIK, I. N., SHAO, Y., MARTICORENA, B. & BERGAMETTI, G. 2009. Development of a physically based dust emission module within the Weather Research and Forecasting (WRF) model: Assessment of dust emission parameterizations and input parameters for source regions in Central and East Asia. Journal of Geophysical Research: Atmospheres, 114.

Dubovik, O. and M. D. King (2000): A flexible inversion algorithm for retrieval of aerosol optical properties from Sun and sky radiance measurements, J. Geophys. Res., 105, 20 673-20 696.

El Amraoui, L., Plu, M.,Guidard, V., Cornut, F., Bacles, M. A Pre-Operational System Based on the Assimilation of MODIS Aerosol Optical Depth in the MOCAGE Chemical Transport Model. RemoteSens. 2022, 1, Accepted

Esselborn M., and A. Schladitz (2012), Atmospheric dust modeling from meso to global scales with the online NMMB/BSC-Dust model - Part 2: Experimental campaigns in Northern Africa, Atmos. Chem. Phys., 12, 2933-2958, doi:10.5194/acp- 12-2933-2012

Forêt, G., Bergametti, G., Dulac, F., and Menut, L. (2006): An optimized particle size bin scheme for modeling mineral dust aerosol, J. Geophys. Res., 111, D17310, doi:10.1029/2005JD006797.

Gasch, P., Rieger, D., Walter, C., Khain, P., Levi, Y., Knippertz, P., and Vogel, B. (2017): Revealing the meteorological drivers of the September 2015 severe dust event in the Eastern Mediterranean, Atmos. Chem. Phys., 17, 13573-13604, https://doi.org/10.5194/acp-17-13573-2017.

Ginoux, P., Chin, M., Tegen, I., Prospero, J. M., Holben, B., Dubovik, O., and Lin, S.J. (2001): Sources and distributions of dust aerosols simulated with the GOCART model, Geophys. Res., 106, 20255-20274 10.1029/2000JD000053.

Giorgi, F. and W. L. Chameides, Rainout Lifetimes of Highly Soluble Aerosols and Gases as Inferred From Simulations With a General Circulation Model, J. Geophys. Res., 91(D13), 367-376, 1986.

Grell, G. A., S. E. Peckham, R. Schmitz, S. A. McKeen, G. Frost, W. C. Skamarock, and B. Eder (2005), Fully coupled 'online' chemistry in the WRF model, Atmos. Environ., 39, 6957–6976, https://doi.org/10.1016/j.atmosenv.2005.04.027.

Guelle, W., Balkanski, Y. J., Schulz, M., Marticorena, B., Bergametti, G., Moulin, C., Arimoto, R., and Perry, K. D. (2000): Modeling the atmospheric distribution of mineral aerosol: Comparison with ground measurements and satellite observations for yearly and synoptic timescales over the North Atlantic, J. Geophys. Res., 105, 1997 -2012.

Guth, J., Josse, B., Marécal, V., Joly, M., and Hamer, P.: First implementation of secondary inorganic aerosols in the MOCAGE version R2.15.0 chemistry transport model, Geosci. Model Dev., 9, 137-160, doi: 10.5194/gmd-9-137-2016, 2016.

Haustein, K., C. Pérez, J. M. Baldasano, O. Jorba, S. Basart, R. L. Miller, Z. Janjic, T. Black, S. Nickovic, M. C. Todd, R. Washington, D. Müller, M. Tesche, B. Weinzierl,

Haustein, K., Pérez, C., Baldasano, J. M., Müller, D., Tesche, M., Schladitz, A., Esselborn, M., Weinzierl, B., Kandler, K. and Hoyningen-Huene, W.V. (2009): Regional dust model performance during SAMUM 2006, J. Geophys. Res. Lett., 36, L03812, doi:10.1029/2008GL036463.

Holben, B.N., T.F. Eck, I. Slutsker, D. Tanré, J.P. Buis, A. Setzer, E. Vermote, J.A. Reagan, Y. Kaufman, T. Nakajima, F. Lavenu, I. Jankowiak, and A. Smirnov (1998): AERONET - A federated instrument network and data archive for aerosol characterization, Rem. Sens. Environ., 66, 1-16.

Hongisto, M. & Sofiev, M. (2004) Long-Range Transport of Dust to the Baltic Sea Region. In: Goos G., Hartmanis J and van Leeuwen J., (ed's) Lecture Notes in Computer Science, Springer-Verlag Berlin Heidelberg, pp. 303-311.

Hortal, M., and Simmons, A.J. (1991): Use of reduced Gaussian grids in spectral models. Mon. Wea. Rev., 119, 1057-1074.

Hsu, N. C., S.-C. Tsay, M. D. King and J. R. Herman (2004): Aerosol Properties Over Bright-Reflecting Source Regions, IEEE Transactions on Geoscience and Remote Sensing, 42, 3, 557-569

Hsu, N. C., S.-C. Tsay, M. D. King and J. R. Herman (2006): Deep Blue Retrievals of Asian Aerosol Properties During ACE-Asia, IEEE Transactions on Geoscience and Remote Sensing, 44, 11, 3180-3195

Huneeus, N., Schulz, M., Balkanski, Y., Griesfeller, J., Kinne, S., Prospero, J., Bauer, S., Boucher, O., Chin, M., Dentener, F., Diehl, T., Easter, R., Fillmore, D., Ghan, S., Ginoux, P., Grini, A., Horowitz, L., Koch, D., Krol, M. C., Landing, W., Liu, X.,

Mahowald, N., Miller, R., Morcrette, J.-J., Myhre, G., Penner, J. E., Perlwitz, J., Stier, P., Takemura, T., and Zender, C. (2010): Global dust model intercomparison in AeroCom phase I, Atmos. Chem. Phys. Discuss., 10, 23781-23864, doi:10.5194/acpd-10-23781-2010.

J. Simmons, M. Suttie, and the GEMS-AER team (2009), Aerosol analysis and forecast in the ECMWF Integrated Forecast System. Part II: Data assimilation, J. Geophys. Res., 114, D13205, doi:10.1029/2008JD011115.

Janjic, Z. I. (1994): The step-mountain eta coordinate model: further developments of the convection, viscous sublayer, and turbulence closure schemes, Mon. Weather Rev., 122, 927-945.

Josse B., Simon P. and V.-H. Peuch, Rn-222 global simulations with the multiscale CTM MOCAGE, Tellus, 56B, 339-356, 2004.

KONTOS, S., LIORA, N., GIANNAROS, C., KAKOSIMOS, K., POUPKOU, A. & MELAS, D. 2018. Modeling natural dust emissions in the central Middle East: Parameterizations and sensitivity. Atmospheric Environment, 190, 294-307.

Lagarde, T., Piacentini, A. and O. Thual, A new representation of data assimilation methods: the PALM flow charting approach, Q.J.R.M.S., 127, 189-207, 2001.

Lahoz, W.A., et al, The Assimilation of Envisat data (ASSET) project, Atmos. Chem. Phys., 7, 1773-1796, 2007.

Lefèvre, F., Brasseur, G. P., Folkins, I., Smith, A. K. and P. Simon, Chemistry of the 1991-1992 stratospheric winter: three-dimensional model simulations, J. Geophys. Res., 99 (D4), 8183-8195, 2004.

LeGrand, S. L., C. Polashenski, T. W. Letcher, G. A. Creighton, S. E. Peckham, and J. D Cetola (2019), The AFWA dust emission scheme for the GOCART aerosol model in WRF-Chem v3.8.1, Geosci. Model Dev., 12, 131–166, https://doi.org/10.5194/gmd-12-131-2019.

Leuenberger D., Koller M., Fuhrer O. and Schär C. (2010): A generalization of the SLEVE vertical coordinate, Mon. Weather Rev. 138: 3683–3689.

LIORA, N., MARKAKIS, K., POUPKOU, A., GIANNAROS, T. M. & MELAS, D. 2015. The natural emissions model (NEMO): Description, application and model evaluation. Atmospheric Environment, 122, 493-504.

Louis J.F., A parametric model of vertical eddy fluxes in the atmosphere, B. Layer Meteor., 17, 197-202, 1979.

Lu et al. (2010): Development of NCEP Global Aerosol Forecasting System: An overview and its application for improving weather and air quality forecasts, NATO Science for Peace and Security Series: Air Pollution Modeling and Its Application XX, 451-454, 2010, doi:10.1007/978-90-481-3812-8.

Lu, C.-H., da Silva, A., Wang, J., Moorthi, S., Chin, M., Colarco, P., Tang, Y., Bhattacharjee, P. S., Chen, S.-P., Chuang, H.-Y., Juang, H.-M. H., McQueen, J., and Iredell, M. (2016): The implementation of NEMS GFS Aerosol Component (NGAC) Version 1.0 for global dust forecasting at NOAA/NCEP, Geosci. Model Dev., 9, 1905-1919, doi:10.5194/gmd-9-1905-2016.

Madronich S., Photodissociation in the atmosphere, 1. Actinic flux and the effects of ground reflections and clouds, J. Geophys. Res., 92, 9740-9752, 1987.

MALM, W. C. & HAND, J. L. J. A. E. 2007. An examination of the physical and optical properties of aerosols collected in the IMPROVE program. 41, 3407-3427.

Marécal, V., Peuch, V.-H., Andersson, C., Andersson, S., Arteta, J., Beekmann, M., Benedictow, A., Bergström, R., Bessagnet, B., Cansado, A., Chéroux, F., Colette, A., Coman, A., Curier, R. L., Denier van der Gon, H. A. C., Drouin, A., Elbern, H., Emili, E., Engelen, R. J., Eskes, H. J., Foret, G., Friese, E., Gauss, M., Giannaros, C., Guth, J., Joly, M., Jaumouillé, E., Josse, B., Kadygrov, N., Kaiser, J. W., Krajsek, K., Kuenen, J., Kumar, U., Liora, N., Lopez, E., Malherbe, L., Martinez, I., Melas, D., Meleux, F., Menut, L., Moinat, P., Morales, T., Parmentier, J., Piacentini, A., Plu, M., Poupkou, A., Queguiner, S., Robertson, L., Rouïl, L., Schaap, M., Segers, A., Sofiev, M., Thomas, M., Timmermans, R., Valdebenito, A., Van Velthoven, P., Van Versendaal, R., Vira J. and Ung A., 2015. A regional air quality forecasting system over Europe: the MACC-II daily ensemble production,Geosci. Model Dev., 8, 2777-2813, doi: 10.5194/gmd-8-2777-2015, 2015.

Mari, C., Jacob, D.J. and Betchold,P., Transport and scavenging of soluble gases in a deep convective cloud, J. Geophys. Res., 105, D17, 22, 255–22267, 2000.

Martet, M., Peuch, V.-H., Laurent, B., Marticorena B. and Bergametti G., evaluation of long-range transport and deposition of desert dust with the CTM Mocage, Tellus, 61B, 449-463, 2009.

Marticorena, B., and Bergametti, G. (1995): Modeling the atmospheric dust cycle: 1. Design of a soil-derived dust emission scheme, Geophys. Res., 100, 6415-16430.

Ménégoz, M., Salas y Melia, D., Legrand, M., Teyssèdre, H., Michou, M., Peuch, V.-H., Martet, M., Josse, B.and Etchevers-Dombrowski, I., Equilibrium of sinks and sources of sulphate over Europe: comparison between a six-year simulation and EMEP observations, Atmos. Chem. Phys., 9, 4505-4519, 2009.

Menut, L. (2008): Sensitivity of hourly Saharan dust emissions to NCEP and ECMWF modeled wind speed, J. Geophys. Res., 113, D16201, doi:10.1029/2007JD009522.

Menut, L., C. Schmechtig, and B. Marticorena (2005), Sensitivity of the sandblasting flux calculations to the soil size distribution accuracy, Journal of Atmospheric and Oceanic Technology, 22(12), 1875-1884.

Menut, L., Forêt, G. and Bergametti, G. (2007): Sensitivity of mineral dust concentrations to the model size distribution accuracy, J. Geophys. Res., 112, D10210, doi:10.1029/2006JD007766.

Menut, L., I. Chiapello and C. Moulin (2009), Previsibility of mineral dust concentrations: The CHIMERE-DUST forecast during the first AMMA experiment dry season , J. Geophys. Res. Atmospheres, 114, D07202, doi: 10.1029/2008JD010523.

Menut, L., Masson, O., and Bessagnet, B. (2009b): Contribution of Saharan dust on radionuclides aerosols activity levels in Europe? The 21-22 February 2004 case study, J. Geophys. Res., 114, D16202, doi:10.1029/2009JD011767.

Michou M., Laville, P., Serça, D., Fotiadi, A., Bouchou, P.and Peuch, V.-H., Measured and modeled dry deposition velocities over the ESCOMPTE area, Atmos. Res., 74 (1-4), 89-116, 2004.

Mishchenko, M. I., L. D. Travis, and A. A. Lacis (2002): Scattering, Absorption, and Emission of Light by Small Particles, Cambridge University Press, Cambridge.

Morcrette, J. J., Boucher, O., Aerosol analysis and forecast in the ECMWF Integrated Forecast System: Forward modelling. J. Geophys. Res., 114, D06206.

Morcrette, J.J., Beljaars, A., Benedetti, A., Jones, L., and Boucher O. (2008): Sea-salt and dust aerosols in the ECMWF IFS. Geophys. Res. Lett., 35, L24813, doi:10.1029/2008GL036041.

Morcrette, J.-J., Boucher, O., Jones, L., Salmond, D., Bechtold, P., Beljaars, A., Benedetti, A., Bonet, A., Kaiser, J.W., Razinger, M., Schulz, M., Serrar, S., Simmons, A.J., Sofiev, M., Suttie, M., Tompkins, A.M., Untch, A., and the GEMS-AER team: (2009): Aerosol analysis and forecast in the ECMWF Integrated Forecast System. Part I: Forward modelling, J. Geophys. Res., 114, D06206, doi:10.1029/2008JD011235.

Nho-Kim, E.-Y., Michou, M. and Peuch, V.-H., Parameterization of size dependent particle dry deposition velocities for global modeling, Atmos. Env., 38 (13), 1933-1942, 2004.

Nho-Kim, E.-Y., Peuch, V.-H. and Oh, S. N. , Estimation of the global distribution of Black Carbon aerosols with MOCAGE, J. Korean Meteor. Soc., 41(4), 587-598, 2005.

Nickovic, S., G. Kallos, A. Papadopoulos and O. Kakaliagou (2001) A model for prediction of desert dust cycle in the atmosphere, J. Geophys. Res., 106, 18113 – 18129.

Nickovic, S., Pejanovic, G., Ozsoy, E., Pérez, C., and Baldasano, J. M. (2004): Interactive Radiation-Dust Model: A Step to Further Improve Weather Forecasts, International Symposium on Sand and Dust Storm, Beijing, China, September 12- 14 .

Noilhan, J. and Planton, S., A simple parameterization of land surface processes for meteorological models, Mon. Wea. Rev., 117, 536-549, 1989.

O'Neill, N. T., Eck, T. F., Smirnov, A., Holben, B. N., and Thulasiraman, S. (2003): Spectral discrimination of coarse and fine mode optical depth, J. Geophys. Res., 108, 4559.

OWEN, P. R. 1964. Saltation of uniform grains in air. Journal of Fluid Mechanics, 20, 225-242.

Pejanovic, G., A. Vukovic, M. Vujadinovic and M. Dacic (2010), Assimilation of satellite information on mineral dust using dynamic relaxation approach. Geophys. Res. Abs., 12, EGU2010-7353.

Pérez C., S. Nickovic, G. Pejanovic, J.M. Baldasano and E. Ozsoy (2006a) Interactive Dust-radiation Modeling: A Step to improve Weather Forecast, J. Geophys. Res., 111, D16206, doi:10.1029/2005JD006717.

Pérez, C., Haustein, K., Janjic, Z., Jorba, O., Huneeus, N., Baldasano, J. M., Black, T., Basart, S., Nickovic, S., Miller, R. L., Perlwitz, J. P., Schulz, M., and Thomson, M. (2011): Atmospheric dust modeling from meso to global scales with the online NMMB/BSC-Dust model–Part 1: Model description, annual simulations and evaluation, Atmos. Chem. Phys., 11, 13001-13027, doi:10.5194/acp-11-13001-2011, 2011.

Perez, C., S. Nickovic, J. M. Baldasano, M. Sicard, F. Rocadenbosch, and V. E. Cachorro (2006b) A long Saharan dust event over the western Mediterranean: Lidar, Sunphotometer observations, and regional dust modeling, J. Geophys. Res., 111, D15214 doi:10.1029/2005JD006579.

PITCHFORD, M., MALM, W., SCHICHTEL, B., KUMAR, N., LOWENTHAL, D., HAND, J. J. J. O. T. A. & ASSOCIATION, W. M. 2007. Revised algorithm for estimating light extinction from IMPROVE particle speciation data. 57, 1326-1336.

Prigent,C., Tegen, I., Aires,F., Marticorena, B., Zribi.M. (2005) Estimation of the aerodynamic roughness length in arid and semi-arid regions over the globe with the ERS

scatterometer, JGR, 110, D09205, doi:10.1029/2004JD005370

RAUPACH, M., GILLETTE, D. & LEYS, J. 1993. The effect of roughness elements on wind erosion threshold. Journal of Geophysical Research: Atmospheres, 98, 3023-3029.

Rieger, D., A. Steiner, V. Bachmann, P. Gasch, J. Förstner, K. Deetz, B. Vogel, and H. Vogel (2017): Impact of the 4 April 2014 Saharan dust outbreak on the photovoltaic power generation in Germany, Atmospheric Chemistry and Physics, 17(21), 13,391–13,415, doi:10.5194/acp-17-13391-2017.

Rieger, D., M. Bangert, I. Bischoff-Gauss, J. Förstner, K. Lundgren, D. Reinert, J. Schröter, H. Vogel, G. Zängl, R. Ruhnke, and B. Vogel (2015): ICON–ART 1.0 – a new online-coupled model system from the global to regional scale, Geosci. Model Dev., 8, 1659–1676, https://doi.org/10.5194/gmd-8-1659-2015.

Schulz M. (2007), Constraining model estimates of the aerosol radiative forcing, Habilitation thesis presented to Université Pierre et Marie Curie, Paris VI, December 2007.

Schulz M., A. Cozic and S. Szopa (2009), LMDzT-INCA dust forecast model developments and associated validation efforts, IOP Conf. Ser.: Earth Environ. Sci. 7 012014, doi:10.1088/1755-1307/7/1/012014.

Schulz, M., Balkanski, Y.J., Guelle, W., and Dulac, F. (1998): Role of aerosol size distribution and source location in a three-dimensional simulation of a Saharan dust episode tested against satellite-derived optical thickness, J. Geophys. Res., 103 (D9), 10579-10592.

Shao, Y. and Lu, H. (2000): A simple expression for wind erosion threshold friction velocity, J. Geophys. Res.-Atmos., 105, 22437–22443, https://doi.org/10.1029/2000JD900304.

Shao, Y., Raupach, M. R., and Findlater, P. A. (1993): Effect of saltation bombardment on the entrainment of dust by wind, J. Geophys. Res., 98, 12719, doi:10.1029/93JD00396.

Sofiev, M., Vira, J., Kouznetsov, R., Prank, M., Soares, J., Genikhovich, E. (2015) Construction of the SILAM Eulerian atmospheric dispersion model based on the advection algorithm of Michael Galperin, Geosci.Model Developm. 8, 3497-3522, doi:10.5194/gmd-8-3497-2015.

Tagliabue, A., L. Bopp and O. Aumont (2009) Evaluating the importance of atmospheric and sedimentary iron sources to Southern Ocean biogeochemistry. Geophys. Res. Lett., 36, L13601, doi:10.1029/2009GL038914

Toon, O.B., and Ackerman, T.P. (1981): Algorithms for the calculation of scattering by stratified spheres. Appl. Opt., 20, 3657-3660.

Vogel, B., Hoose, C., Vogel, H., and Kottmeier, C. (2006): A model of dust transport applied to the Dead Sea Area, Meteorol. Z., 15, 611–624, https://doi.org/10.1127/0941-2948/2006/0168.

Vuolo, M.R., Chepfer, H. Menut, L., and Cesana, G. (2009): Comparison of mineral dust layers vertical structures modelled with CHIMERE-DUST and observed with the CALIOP lidar, J. Geophys. Res., Vol. 114, D09214, doi:10.1029/2008JD011219.

Weinzierl, B.B. (2007) Radiatively-driven processes in forest fire and desert dust plumes. Dissertation an der Fakultät für Physik der Ludwig-Maximilians-Universität München. Munchen, 2007.

White, B. R. (1979): Soil transport by winds on Mars, J. Geophys. Res.-Sol.Ea., 84, 4643–4651, https://doi.org/10.1029/JB084iB09p04643.

Woodward, S. (2001) Modeling the atmospheric life cycle and radiative impact of mineral

dust in the Hadley Centre climate model, J. Geophys. Res., 106, D16, doi: 10.1029/2000JD900795.

Woodward, S. (2011) Mineral dust in HadGEM2, Tech. Note 87, Hadley Cent., Met Office, Exeter, UK.

Xie, J., C. Yang, G. Pejanovic, B. Zhou and Q. Huang (2008) Utilize multi CPU cores to improve dust simulation performance, Eos Trans. AGU, 89(53), Fall Meet. Suppl., Abstract: IN23C-1103.

Zakey, A. S., F. Solmon, and F. Giorgi, (2006): Implementation and testing of a desert dust module in a regional climate model, Atmos. Chem. Phys., 6, 4687-4704.

Zängl, G., D. Reinert, R. P., and B. M. (2015): The ICON (ICOsahedral Non-hydrostatic) modelling framework of DWD and MPI-M: Description of the non-hydrostatic dynamical core, Quarterly Journal of the Royal Meteorological Society, 141(687), 563–579, doi:10.1002/qj.2378.

Zender, C.S., Bian, H., Newman, D. (2003) Mineral Dust Entrainment and Deposition (DEAD) model: Description and 1990s dust climatology. JGR, 108. D14, 4416, doi:10.1029/2002JD002775.

7. Appendices

7.1. Appendix A: Models description

7.1.1. BSC-DREAM8b

Model	BSC-DREAM8b v2.0
Institution	BSC
Meteorological driver	Eta/NCEP
Domain of simulation	0-65ºN and 26ºW-60ºE
Meteorological initial fields	NCEP (GFS)
Emission scheme	Dust uplifting following Shao et al. (1993) using the USGS global 1-km land cover data is used to specify dust productive model points. Include the *viscous sublayer* approach between the surface and the lowest model layer (Janjic, 1994). This updated version (v2.0) includes a preferential source mask based on Ginoux et al. (2001) in its emission scheme.
Time step	120 s
Horizontal resolution	1/3º x 1/3º
Vertical resolution	24 Eta-layers
Height first layer	86 m (above sea level)
Radiation interactions	Radiation feedbacks described in Pérez et al. (2006a)
Transport size bins	8 bins (0.1-10μm)
Data assimilation	No
Model original coordinates	Eta rotated grid.
Dust outputs parameters	
LOAD_DUST	Total dust concentration for the entire atmospheric column of the model. Directly from the model outputs.
SCONC_DUST	Total dust concentration present in the first model layer above the topography. Directly from the model outputs.
AOD550_DUST	Dust AOD is related to column mass loading by: $AOD(\lambda)=\sum_{1}^{8} AOD_k(\lambda)=\sum_{1}^{8} \frac{3}{4\rho_k r_k} M_k Q_{ext}(\lambda)_k$ where for each size bin *k*: ¤*k* is the particle mass density, *rk* is the effective radius, *Mk* is the column mass loading and *Qext*(λ)*k* is the extinction efficiency factor which was calculated using Mie scattering theory and we have considered the dust refraction indices from OPAC database. The Mie code used has been described in Mischenko et al. (2002).
Model output	File format: NetCDF Grid: Regular Lat-Lon. Linear interpolation. Longitude: 256 grid points (0-65ºN vector in inc = 1/3º) Latitude: 196 grid points (26ºW-60ºE vector in inc = 1/3º) Time: 3-hourly vector starting at 12UTC (with 72h dust forecast) Variables: *LOAD_DUST, SCONC_DUST, OD550_DUST, EMI_DUST*
References	Nickovic et al. (2001), Pérez et al. (2006a,b), Haustein et al. (2009)

7.1.2. CHIMERE

Model	CHIMERE
Institution	LMD
Meteorological driver	WRF
Domain of simulation	North-Atlantic (including Europe and Africa): 100°W -80°E and 5°S -65°N
Meteorological initial fields	NCEP (GFS)
Emission scheme	Marticorena and Bergametti (1995) for saltation. Alfaro and Gomez (2011) (with update of Menut et al., 2005) for sandblasting.
Time step	5mn
Horizontal resolution	1° x 1°
Vertical resolution	30 levels from surface to 200hPa
Height first layer	~40m (above the surface, but coordinates in sigma/pressure, depends on the location and meteorology)
Radiation interactions	No.
Transport size bins	9 bins (mean median diameter from 0.039 to 20µm).
Data assimilation	No.
Model original coordinates	Regular lat/lon.
Dust outputs parameters	
LOAD_DUST	Total dust concentration for the entire atmospheric column of the model. Directly from the model outputs.
SCONC_DUST	Total dust concentration present in the first model layer.
AOD550_DUST	Mass column loading used with a Mie code to compute.
EMI_DUST	Emissions fluxes in $g/cm^2/day$
Model output	File format: NetCDF Grid: Regular Lat-Lon. Longitude: 181 grid points (100°W-80°E) Latitude: 71 grid points (5°S-65°N) Time: Hourly outputs with 72h dust forecast starting at 00 of [D-1] Variables: *LOAD_DUST, SCONC_DUST, OD550_DUST, EMI_DUST*
References	Forêt et al. (2006), Menut (2008), Menut et al. (2005, 2007, 2008, 2009a,b), Vuolo et al. (2009)

7.1.3. LMDzT-INCA

Model	LMDzT-INCA
Institution	LSCE
Meteorological driver	LMDzT
Domain of simulation	Global
Meteorological initial fields	ECMWF-IFS
Emission scheme	Dust uplifting following Schulz et al. (1998), Guelle et al., (2000), Schulz (2007) using soil texture, soil humidity, maps of potential source strength and threshhold velocity derived from FAO soil maps.
Time step	30 minutes
Horizontal resolution	3.75° x 2.85°
Vertical resolution	19 sygma-hybrid-layers
Height first layer	120 m (above surface)
Radiation interactions	No in forecast mode (potentially yes)
Transport size bins	1- log normal mode, mass and number (width 2, MMD 1.5-2.5 µm)
Data assimilation	No
Model original coordinates	regular Lat-Lon
Dust outputs parameters	
LOAD_DUST	Directly from model output
SCONC_DUST	Directly from model output
AOD550_DUST	Dust AOD is function of local MMD, refractive index and aerosol mass.
Model output	File format: NetCDF Grid: Regular Lat-Lon Longitude: as documented in netCDF file Latitude: as documented in netCDF file, 1/2 degree at poles Time: 3-hourly for 72 hours into future starting at 00UTC. Variables: *LOAD_DUST, SCONC_DUST, OD550_DUST, EMI_DUST*
References	Balkanski et al. (2006), Huneeus et al. (2011), Guelle et al. (2000), Schulz (2007) , Schulz et al. (1998, 2009)

7.1.4. CAMS

Model	CAMS
Institution	ECMWF
Meteorological driver	ECMWF
Domain of simulation	Global
Meteorological initial fields	ECMWF/IFS
Emission scheme	Dust uplifting following Ginoux et al. (2001) and Morcrette et al. (2008, 2009).
Time step	1800s
Horizontal resolution	8-10 km approx. (O1280)
Vertical resolution	137 ¤-layers
Height first layer	10 m (above the surface)
Radiation interactions	No.
Transport size bins	3 bins (0.03 - 0.55 - 0.9 - 20¤m)
Data assimilation	Yes. (Benedetti et al., 2009)
Model original coordinates	IFS reduced-Gaussian grid (Hortal and Simmons, 1991)
Dust outputs parameters	
LOAD_DUST	Total dust concentration for the entire atmospheric column of the model. Directly from the model outputs.
SCONC_DUST	Total dust concentration present in the first model layer above the topography. Directly from the model outputs.
AOD550_DUST	Dust AOD is related to column mass loading and the dust refraction indices from Kinne. The Mie code used has been described in Toon and Ackerman (1981).
Model output	File format: NetCDF Grid: Regular Lat-Lon. Linear interpolation to 1° x 1° Longitude: 360 grid points Latitude: 180 grid points Time: 3-hourly vector starting at 00UTC Variables: *LOAD_DUST, SCONC_DUST, OD550_DUST, EMI_DUST*
References	Benedetti et al. (2008), Hortal et al. (2009), Morcrette et al. (2008, 2009)

7.1.5. DREAM8-NMMB-MACC

Model	DREAM8-NMME-MACC
Institution	SEEVCCC
Meteorological driver	NMME
Domain of simulation	0-60ºN and 25ºW-45ºE
Meteorological initial fields	ECMWF
Emission scheme	Dust uplifting following Shao et al. (1993) using the USGS global 1-km land cover data is used to specify dust productive model points. Include the viscous sublayer approach between the surface and the lowest model layer (Janjic, 1994).
Time step	120 s
Horizontal resolution	1/3º x 1/3º
Vertical resolution	28 hybrid layers
Height first layer	48 m above sea level (approx.)
Radiation interactions	No at the moment
Transport size bins	8 bins (0.1-10μm)
Data assimilation	ECMWF-dust-analysis at 18:00 UTC is used as a target field to which 6-hour nudging is done with Newtonian relaxation assimilation.
Model original coordinates	Eta rotated grid.
Dust outputs parameters	
LOAD_DUST	Total dust concentration for the entire atmospheric column of the model. Directly from the model outputs.
SCONC_DUST	Total dust concentration present in the first model layer above the topography. Directly from the model outputs.
AOD550_DUST	Dust AOD is related to column mass loading by: $AOD(\lambda)=\sum_{1}^{8} AOD_k(\lambda)=\sum_{1}^{8} \frac{3}{4\rho_k r_k} M_k Q_{ext}(\lambda)_k$ where for each size bin *k*: ¤*k* is the particle mass density, *rk* is the effective radius, *Mk* is the column mass loading and *Qext*(λ)*k* is the extinction efficiency factor which was calculated using Mie scattering theory and we have considered the dust refraction indices from OPAC database. The Mie code used has been described in Mischenko et al. (2002).
Model output	File format: NetCDF, GRIB Grid: Regular Lat-Lon. Bi-linear interpolation. Longitude: 481 grid points (5-60ºN vector in inc = 1/4º) Latitude: 251 grid points (50ºW-70ºE vector in inc = 1/4º) Time: 3-hourly vector starting at 12UTC (with 72h dust forecast) with one day delay, depends on ECMWF-dust-analysis availability Variables: *LOAD_DUST, SCONC_DUST, AOD550_DUST, EMI_DUST*
References	Nickovic et al. (2001), Nickovic (2004), Benedeti et al, (2008), Pejanovic et al (2010), Xie et al. (2008)

7.1.6. NMMB-MONARCH

Model	NMMB-MONARCH (the mineral dust module is also known as NMMB/BSC-Dust)
Institution	BSC
Meteorological driver	NMMB/NCEP
Domain of simulation	10ºS-66ºN and 33ºW-68ºE
Meteorological initial fields	NCEP (GFS)
Emission scheme	Dust uplifting following Marticorena and Bergametti (1995) using the USGS global 1-km land cover database, the high resolution NESDIS 5-years monthly climatology of vegetation fraction, and topographic preferential source mask of Ginoux to specify dust productive model points. Include the *viscous sublayer* approach between the surface and the lowest model layer (Janjic, 1994).
Time step	80 s
Horizontal resolution	1/3º x 1/3º
Vertical resolution	24 hybrid pressure-sygma layers
Height first layer	108 m (above sea level)
Radiation interactions	Radiation feedbacks described in Pérez et al. (2006a), not activated
Transport size bins	8 bins (0.1-10μm)
Data assimilation	No
Model original coordinates	NMMB rotated grid.
Dust outputs parameters	
LOAD_DUST	Total dust concentration for the entire atmospheric column of the model. Directly from the model outputs.
SCONC_DUST	Total dust concentration present in the first model layer above the topography. Directly from the model outputs.
AOD550_DUST	Dust AOD is related to column mass loading by: $AOD(\lambda)=\sum_{1}^{8} AOD_k(\lambda)=\sum_{1}^{8} \frac{3}{4\rho_k r_k} M_k Q_{ext}(\lambda)_k$ where for each size bin *k*: ¤*k* is the particle mass density, *rk* is the effective radius, *Mk* is the column mass loading and *Qext*(λ)*k* is the extinction efficiency factor which was calculated using Mie scattering theory and we have considered the dust refraction indices from OPAC database. The Mie code used has been described in Mischenko et al. (2002).
Model output	File format: NetCDF Grid: Regular Lat-Lon. Linear interpolation. Longitude: 289 grid points (10ºS-66ºN vector in inc = 1/3º) Latitude: 211 grid points (33ºW-68ºE vector in inc = 1/3º) Time: 3-hourly vector starting at 12UTC (with 72h dust forecast) Variables: *SCONC_DUST, OD550_DUST*
References	Pérez et al. (2011), Haustein et al. (2011)

7.1.7. MetUM

Model	MetUM^{TM} (global NWP configuration of Met Office Unified Model)
Institution	UK Met Office
Meteorological driver	MetUM
Domain of simulation	Global (but data provided over sub-domain: 60W to 55E,0 to 70N)
Meteorological initial fields	MetUM
Emission scheme	Simplified 2-bin version of Woodward et al. (2001, 2011). Horizontal flux is calculated across 9 bins (0.03-1000 μm) as in Woodward (2011) but vertical flux is emitted into 2 bins only using a prescribed size distribution (instead of the original 6 bins).
Time step	10 mins
Horizontal resolution	0.3516°x0.2344°
Vertical resolution	70 levels from surface to 80km (uses terrain-following staggered Charney- Phillips grid)
Height first layer	~ 20m (theta) and ~10 m (u,v,p,ρ) above surface
Radiation interactions	No (possible but not currently activated).
Transport size bins	2 bins (0.1-2μm, 2-10μm)
Data assimilation	MODIS/Aqua
Model original coordinates	Regular lat-lon
Dust outputs parameters	
SCONC_DUST	Total dust concentration present in the first model layer. Directly from the model outputs.
AOD550_DUST	Mass column loading used with a Mie code (offline) to compute dust extinction coefficients. Dust refractive indices are taken from Balkanski et al (2007).
Model output	File format: NetCDF Grid: Regular Lat-Lon. Longitude: 327 grid points Latitude: 299 grid points Time: 3-hourly vector starting at 00UTC Variables (currently providing): *SCONC_DUST, OD550_DUST*
References	Woodward, S (2011), Mineral dust in HadGEM2, Tech. Note 87, Hadley Cent., Met Office, Exeter, UK. Woodward, S. (2001), Modeling the atmospheric life cycle and radiative impact of mineral dust in the Hadley Centre climate model, *J. Geophys. Res.*, 106, D16, doi:10.1029/2000JD900795

7.1.8. GEOS-5

Model	GEOS-5 Earth System Model
Institution	NASA/Goddard Space Flight Center/Global Modeling and Assimilation
Meteorological driver	Aerosols are transported within the GEOS-5 global model
Domain of simulation	Global
Meteorological initial fields	GEOS-5 Atmospheric Data Assimilation System
Emission scheme	Based on Ginoux (2001)
Time step	Aerosol tendencies computed every 30 minutes
Horizontal resolution	0.25 degree longitude by 0.3125 degree latitude
Vertical resolution	72 vertical layers, model top at 0.01 hPa (~85 km)
Height first layer	
Radiation interactions	Aerosol direct effects on radiation fully included.
Transport size bins	5 bins centered at (0.73 μm, 1.4 μm , 2.4 μm, 4.5 μm, 8.0 μm)
Data assimilation	Data sources: MODIS Aqua/Terra reflectances, Neural Net AOD retrieval Analysis algorithm: 3-hourly analysis splitting consisting of a 2D AOD analysis and 3D increments based on local displacement ensembles.
Model original coordinates	Constant longitude/latitude grid; shortly switching to cubed-sphere
Dust outputs parameters	
DUSMASS	dust surface mass concentration. Dust concentration, summed over the 5 bins, for the first model layer above the surface
DUEXTTAU	dust extinction aot [550 nm]. Computed online based on mass extinction coefficients look up tables. Optical properties based on Colarco et. al. (2002), Kim et al. (2011) and Levoni et al. (1997). Spheroidal shape distribution after Dubovik et al. (2006), properties calculated after Meng et al. (2010).
Model output	File format: COARDS (CF 1.0) compliant NetCDF-4 files Grid: Regular Lat-Lon. Longitude: 1152 grid points (180W-179.6875E, increment: 0.3125°) Latitude: 721 grid points (90S-90N, increment: 0.25 deg) Time: hourly vector starting at 0UTC (with 5 day dust forecast) Variables: *SCONC_DUST, OD550_DUST*
References	Colarco, P., A. da Silva, M. Chin and T. Diehl, 2009: Online simulations of global aerosol distributions in the NASA GEOS-4 model and comparisons to satellite and ground-based aerosol optical depth. *J. Geophys. Res.*, 115, D14207, doi:10.1029/2009JD012820. Nowottnick, E., P. Colarco, A. da Silva, 2011: The Fate of Saharan Dust Across the Atlantic and Implications for a Central Americal Dust Barrier. *Atmos. Chem. Phys.*, 11, 8415-8431, doi:10.5194/acp-11-8415-2011.

7.1.9. NGAC

Model	NCEP NEMS GFS Aerosol Component (NGAC)
Institution	NOAA NCEP
Meteorological driver	NEMS GFS
Domain of simulation	Global
Meteorological initial fields	NCEP GDAS
Emission scheme	Dust uplifting following Ginoux (2001)
Time step	450 seconds
Horizontal resolution	T126 (~ 1 deg)
Vertical resolution	64 vertical sigma-pressure hybrid layers, model top at 0.2 hPa
Height first layer	~ 20 m
Radiation interactions	Aerosol direct effects on radiation not currently activated
Transport size bins	5 bins centered at (0.73 μm, 1.4 μm , 2.4 μm, 4.5 μm, 8.0 μm)
Data assimilation	No
Model original coordinates	GFS reduced Gaussian grids
Dust outputs parameters	
DUSMASS	dusmass dust surface mass concentration. Dust concentration, summed over the 5 bins, for the first model layer above the surface
DUEXTTAU	dust extinction aod [550 nm]. Computed offline based on mass extinction coefficients look up tables.
Model output	File format: GRIB2 Grid: Regular lat-lon. Linear interpolation to 1° x 1° Longitude:360 grid points, Latitude: 180 grid points Time: 3-hourly vector starting at 0UTC (with 5 day dust forecast). Variables: *SCONC_DUST, AOD550_DUST*
References	Lu et al., 2010: Development of NCEP Global Aerosol Forecasting System: An overview and its application for improving weather and air quality forecasts, NATO Science for Peace and Security Series: Air Pollution Modeling and Its Application XX, 451-454, doi:10.1007/978-90-481-3812-8. Lu, C.-H., da Silva, A., Wang, J., Moorthi, S., Chin, M., Colarco, P., Tang, Y., Bhattacharjee, P. S., Chen, S.-P., Chuang, H.-Y., Juang, H.-M. H., McQueen, J., and Iredell, M. (2016): The implementation of NEMS GFS Aerosol Component (NGAC) Version 1.0 for global dust forecasting at NOAA/NCEP, Geosci. Model Dev., 9, 1905-1919, doi:10.5194/gmd-9-1905-2016.

7.1.10. EMA RegCM4

Model	EMA-RegCM4
Institution	EMA
Meteorological driver	Online dust scheme with the Regional Climate Model version 4 (RegCM4)
Domain of simulation	Regional
Meteorological initial fields	NCEP/GFS
Emission scheme	Saltation and sandblasting process (A.S. Zakey 2006), the dust scheme depends on (Marticorena and Bergametti, 1995; Alfaro and Gomes, 2001)
Time step	150 s
Horizontal resolution	45 km x 45 km
Vertical resolution	18 sygma-layers
Height first layer	50 m
Radiation interactions	Yes (both with shortwave and long waves) (Direct effects)
Transport size bins	4 bins(0.01:1 - 1:2.5 - 2.5:5 - 5:20)
Data assimilation	No
Model original coordinates	Arakawa-Lamb B-staggering
Dust outputs parameters	
LOAD_DUST	Total dust concentration for the entire atmospheric column of the model. Directly from the model outputs.
SCONC_DUST	Total dust concentration present in the first model layer above the topography. Directly from the model outputs.
OD550_DUST	AOD is related to column mass loading and the considered dust refraction indices from Kinne. The Mie code used has been described in Toon and Ackerman (1981).
Model output	File format: NetCDF Grid: Lambart Conformal projection Longitude: 240 grid points Latitude: 180 grid points Time: 3-hourly vector starting at 03UTC Variables: *LOAD_DUST, SCONC_DUST, OD550_DUST*
References	A. S. Zakey, F. Solmon, and F. Giorgi, (2006) “Implementation and testing of a desert dust module in a regional climate model”, Atmos. Chem. Phys., 6, 4687-4704.

7.1.11. DREAMBOL

Model	DREAMABOL v1.0
Institution	CNR-ISAC
Meteorological driver	BOLAM
Domain of simulation	0-65ºN and 25ºW-60ºE
Meteorological initial fields	NCEP (GFS)
Emission scheme	Dust uplift following Tegen et al. (1994) using the USGS global 1-km land cover data to specify dust productive model points and FAO soil database for availability of uplifted species. Uses surface TKE based uplift velocity to account for strong convective conditions. Includes a preferential source mask based on Ginoux et al. (2001).
Time step	240 s
Horizontal resolution	0.4º x 0.4º in rotated pole lon-lat grid.
Vertical resolution	50 sygma-hybrid-levels, up to 0.01 hPa
Height first layer	27 m (above surface) at sea level.
Radiation interactions	Based on the substitution of climatological values with the actual model dust AOD in the radiation scheme by Morcrette (1991). Not yet active in operational mode.
Transport size bins	8 bins (0.1-10 μm)
Data assimilation	No
Model original coordinates	Rotated pole lon-lat grid: north_pole_longitude = -162.5, north_pole_latitude=57.5.
Dust outputs parameters	
LOAD_DUST	Total dust concentration for the entire atmospheric column of the model. Directly from the model output.
SCONC_DUST	Total dust concentration present in the first model layer above the topography. Directly from the model output.
EMI_DUST	Emissions fluxes sampled at the output time step (not cumulated). Directly from the model output.
OD550_DUST	Computed run-time, level-by-level, using an approximation of Mie theory (Evans and Fournier, 1990) to compute the extinction coefficient and approximating of the actual particle distribution by a lognormal distribution with the same parameters.
Model output	File format: NetCDF. Grid: model output is interpolated onto the Model Ensemble grid: Longitude: 171 grid points (0-65ºN vector in inc = 0.5º), Latitude: 131 grid points (25ºW-60ºE vector in inc = 0.5º). Time: 3-hourly steps starting at 00UTC (72h forecast) Variables: *LOAD_DUST, SCONC_DUST, OD550_DUST, EMI_DUST*

7.1.12. WRF-CHEM

Model	WRF-CHEM
Institution	NOA
Meteorological driver	WRF
Domain of simulation	2-70°N and 28°W-66°E
Meteorological initial fields	GFS
Emission scheme	Gocart scheme by Ginoux et al. (2001)
Time step	60 s
Horizontal resolution	0.19° x 0.22°
Vertical resolution	30 sigma levels
Height first layer	
Radiation interactions	No at the moment
Transport size bins	8 bins (0.15, 0.25, 0.45, 0.78, 1.3, 2.2, 3.8, 7.1μm)
Data assimilation	No
Model original coordinates	Lon-lat standard grid.
Dust outputs parameters	
LOAD_DUST	Total dust concentration for the entire atmospheric column of the model. Directly from the model outputs.
SCONC_DUST	Total dust concentration present in the first model layer above the topography. Directly from the model outputs.
OD550_DUST	Dust AOD is related to column mass loading and considered dust refraction indices.
Model output	File format: NetCDF Grid: Regular Lat-Lon. Longitude: 424 grid points Latitude: 348 grid points Time: 3-hourly vector starting at 12UTC (with 72h dust forecast) Variables: *SCONC_DUST*, *OD550_DUST*
References	In preparation

7.1.13. SILAM

Model	SILAM
Institution	Finnish Meteorological Institute
Meteorological driver	ECMWF/IFS
Domain of simulation	Global -to- γ-mesoscale. Dust forecasts are provided from the global domain
Meteorological initial fields	ECMWF/IFS
Emission scheme	Saltation and sandblasting following Marticorena & Bergametti, (1995), Zender, (2003) with several updates. The sandblasting efficiency is refitted from original Gillette (1979) observations. Critical u* equation was reanalyzed, variables split and an approximate analytical solution found, Size spectrum is after Weinzierl (2007), roughness length is from wind scatterometer after Prigent et al., (2007)
Time step	1200s
Horizontal resolution	0.5° x 0.5°
Vertical resolution	29 hybrid ¤-pressure layers
Height first layer	~25 m (above the surface at the sea level)
Radiation interactions	No.
Transport size bins	5 bins (0.1-1, 1-2.5, 2.5-10, 10-30 μm)
Data assimilation	No
Model original coordinates	Regular lon-lat
Dust outputs parameters	
LOAD_DUST	Total dust concentration for the entire atmospheric column of the model. Directly from the model outputs. Post-processing, available on request.
CONC_DUST	Total dust concentration in the first model layer. Available as a layer of a 3D field directly from the model outputs.
OD550_DUST	AOD is related to column mass loading and the dust refraction indices from Kinne. The Mie code used has been described in Toon and Ackerman (1981). AOD of each mode available from model outputs. Total dust AOD is a result of post-processing.
EMI_DUST	Dust emission in kg/cell. Can be enabled in the model outputs on request.
Model output	File format: NetCDF4 Grid: Regular Lat-Lon. 0.5° x 0.5° Longitude: 720 grid points Latitude: 359 grid points Time: hourly-averaged, starting at 00UTC up to +120 hours Variables: *LOAD_DUST, CONC_DUST, OD550_DUST, EMI_DUST*
References	Sofiev et al (2015), Hongisto & Sofiev, (2005). Description of the current dust emission scheme is under preparation

7.1.14. LOTOS-EUROS

Model	LOTOS-EUROS
Institution	TNO
Meteorological driver	ECMWF
Domain of simulation	0-65 ºN and 25ºW-65ºE
Meteorological initial fields	ECMWF
Emission scheme	GLC land cover map, STATSGO soil texture map, potential sources approach by Ginoux et al (2001). Approach by Marticorena& Bergametti 1995, impact of clay fraction by Fécan et al (1999) with modification as in Mokthari et al (2012). Dust uplifting following Shao et al. (2001).
Time step	Variable, depends on Courant conditions
Horizontal resolution	1/2º x 1/4º (lon x lat)
Vertical resolution	4 dynamical layers + surface layer
Height first layer	25 m above terrain
Radiation interactions	No
Transport size bins	5 bins (0.1-10µm)
Data assimilation	no
Model original coordinates	Regular lon-lat
Dust outputs parameters	
SCONC_DUST	Translation of dust in first model layer to observation height (2.5 m above terrain) using constant flux approach (direct model output)
OD550_DUST	AOD is calculated per layer based on mass extinction coefficents for concentrations per size bin, then summed to obtain total column AOD
Model output	File format: NetCDF Grid: Regular Lat-Lon. Time: 3-hourly vector starting at 00 UTC (with 72h dust forecast) with one day delay, depends on ECMWF-dust-analysis availability Variables: *SCONC_DUST, OD550_DUST*
References	LOTOS-EUROS v2.0 reference guide, 2016 A.M.M. Manders and S. Janson, *Modelling of mineral dust in the Sahara region*, TNO report TNO2014 R11118, 2014 Both available at www.lotos-euros.nl

7.1.15. ICON-ART

Model	ICON-ART
Institution	DWD + KIT
Meteorological driver	DWD
Domain of simulation	Global with two-way nest (0 -82°N,68°W-68°E)
Meteorological initial fields	From own data assimilation cycle
Emission scheme	Saltation and threshold friction velocity for dust emission flux; HWSD for soil types (Rieger et al., 2017; Vogel et al., 2006; White, 1979; Shao and Lu, 2000; Alfaro and Gomes, 2001)
Time step	Global: 6 minutes, nest: 3 minutes
Horizontal resolution	40 km global + 20 km two-way nest over Europe, North Atlantic and North Africa. Triangular mesh based on an icosahedron.
Vertical resolution	90 (global) and 60 (nest) Smooth Level Vertical SLEVE coordinate (Leuenberger 2010)
Height first layer	10 m (above the surface) for global and nest
Radiation interactions	Radiation feedback (direct and semi-direct effect) described in Rieger et al. (2017) and in Gasch et al. (2017)
Transport size bins	3-log normal modes for mass and number concentration
Data assimilation	Yes, same observations as in operational ICON at DWD. Prognostic dust is included in first guess of DA cycle, but so far no assimilation of dust observations is done.
Model original coordinates	Triangular grid
Dust outputs parameters	
SCONC_DUST	Total dust mass concentration present in the first model layer above the topography.
OD550_DUST	AOD is calculated per layer based on mass extinction coefficients for mass concentrations per mode, then summed to obtain total column AOD.
Model output	File format: NetCDF Grid: Regular Lat-Lon of nest region. Linear interpolation to 1/16° x 1/16° Longitude: 1041 grid points Latitude: 1361 grid points Time: 6-hourly vector starting at 00 UTC Variables: SCONC_DUST, OD550_DUST
References	Rieger et al. (2017), Gasch et al. (2017), Rieger et al. (2015), Zängl et al. (2015), Vogel et al. (2006)

7.1.16. DREAM8-NMME-MSG

Model	DREAM-NMME-MSG
Institution	IAASARS/NOA
Meteorological driver	NMME
Domain of simulation	0°-55°N , 40°W -80°E
Meteorological initial fields	NCEP/GFS
Emission scheme	Dust uplifting following Shao et al. (1993) and Nickovic et al., 2001. Includes the viscous sublayer approach between the surface and the lowest model layer (Janjic, 1994).
Time step	72 s
Horizontal resolution	1/5° x 1/5°
Vertical resolution	28 hybrid layers
Height first layer	50 m above sea level (approx.)
Radiation interactions	No
Transport size bins	8 bins (0.1-10μm)
Data assimilation	MSG-SEVIRI at 12:00 UTC is used as a target field to which 6-hour nudging is done with Newtonian relaxation assimilation (Pejanovic et al, 2010; Solomos et al., 2017)
Model original coordinates	Eta rotated grid.
Dust outputs parameters	
SCONC_DUST	Total dust concentration present in the first model layer above the topography. Directly from the model output.
OD550_DUST	The dust optical depth is related to column mass loading by: $AOD(\lambda)=\sum_{1}^{8} AOD_k(\lambda)=\sum_{1}^{8}\frac{3}{4\rho_k r_k} M_k Q_{ext}(\lambda)_k$ where for each size bin k: ρk is the particle mass density, rk is the effective radius, Mk is the column mass loading and Qext(λ)k is the extinction efficiency factor which was calculated using Mie scattering theory and we have considered the dust refraction indices from OPAC database. The Mie code used has been described in Mischenko et al. (2002).
Model output	NetCDF Regular Lat-Lon. Bi-linear interpolation. Longitude: 701 grid points (5°S-70°N vector in inc = 1/5°) Latitude: 370 grid points (50°W-90°E vector in inc = 1/5°) 3-hourly vector starting at 06UTC (with 72h dust forecast) with one day delay, depends on MSG-SEVIRI dust optical depth availability Variables: *SCONC_DUST, OD550_DUST*
References	Nickovic et al. (2001), Pejanovic et al (2010), Solomos et al. (2017)

7.1.17. ALADIN-Dust

Model	ALADIN-Dust
Institution	ONM-Algeria (ALADIN consortium)
Meteorological driver	ALADIN
Domain of simulation	Regional
Meteorological initial fields	ARPEGE
Emission scheme	The dust fluxes are calculated using the Dust Entrainment And Deposition (DEAD) model (Zender et al., 2003). The physical parameterizations in the DEAD scheme are based on the Marticorena and Bergametti (1995) scheme, in which dust is calculated as a function of saltation and sandblasting. DEAD was implemented in the ISBA scheme embedded in SURFEX (Grini et al., 2006). Recently this emission parameterization has been improved by Mokhtari et al. (2012) in order to better account for the soil aggregate distribution.
Time step	420s
Horizontal resolution	25km x 25km
Vertical resolution	70 σ-layers
Height first layer	65m (approx.)
Radiation interactions	Yes, the Fouquart and Morcrette radiation scheme (FMR;. Morcrette, 1989).
Transport size bins	Log-normal (mode, mass and number) with 3 bins (0.078-5μm)
Data assimilation	No
Model original coordinates	ALADIN rotated grid
Dust outputs parameters	
SCONC_DUST	Total dust concentration present in the first model level, directly from the model outputs.
OD550_DUST	Mass column loading used with a Mie code to compute.
Model output	File format: FA (Form ARPEGE), converted to NetCDF to meet SDSWAS technical requirements. Grid: Regular Lat-Lon Longitude: 342 grid points Latitude: 262 grid points Time: 3-hourly vector starting at 00UTC (with 72h dust forecast) Variables provided: SCONC_DUST, OD550_DUST
References	Zender et al. (2003), Grini et al. (2006), Mokhtari et al. (2012), Mokhtari et al. (2015), P. Termonia et al. (2018).

7.1.18. WRF-NEMO-CAMx

Model	WRF-N.E.MO.-CAMx
Institution	Aristotle University of Thessaloniki
Meteorological driver	WRF
Domain of simulation	37.5ºW-78ºE and 12-60ºN
Meteorological initial fields	NCEP (GFS)
Emission scheme	Horizontal mass flux of Owen (1964), threshold friction velocity from Marticorena and Bergametti (1995), drag partition of Raupach et al. (1993) as in Darmenova et al. (2009) and sandblasting efficiency of Alfaro and Gomes (2001).¤
Time step	Variable, depending on CFL criterion
Horizontal resolution	18km
Vertical resolution	18 layers up to 100hPa
Height first layer	30 m above ground level (approx.)
Radiation interactions	No
Transport size bins	2 bins (0.036-2.5 μm and 2.5-10 μm in diameter)
Data assimilation	No
Model original coordinates	Lambert Conformal Conic
Dust outputs parameters	
SCONC_DUST	Total dust mass concentration present in the first model layer.
OD550_DUST	Calculated (offline) from dust load, applying the mass extinction efficiencies from IMPROVE algorithm (Malm and Hand, 2007, Pitchford et al., 2007).
Model output	NetCDF Regular Lat-Lon. Distance-weigthed interpolation. Longitude: 525 grid points (25ºW-60ºE vector in inc = 0.162º) Latitude: 297 grid points (16ºN-60ºN vector in inc = 0.162º) 1-hourly vector starting at 00UTC (with 72h dust forecast) Variables: SCONC_DUST, OD550_DUST, LOAD_DUST
References	Liora et al. (2015), Kontos et al. (2018)

7.1.19. ZAMG-WRF-CHEM

Model	*WRF-Chem*
Institution	*ZAMG*
Meteorological driver	*WRF, online-coupled model with IFS forecasts used as initial and boundary conditions (3-hourly resolution)*
Domain of simulation	*Regional domain (0-65°N, 25°W-65°E)*
Meteorological initial fields	*IFS forecasts*
Emission scheme	*AFWA dust emission scheme for the GOCART aerosol model (LeGrand et al. 2019), tuning factors for friction velocity, soil moisture, preferential dust source term, and bulk vertical dust emission flux activated*
Time step	*90 seconds*
Horizontal resolution	*0.2° latitude x 0.2° longitude*
Vertical resolution	*47 vertical eta levels, model top at 50 hPa*
Height first layer	*~25 m above the surface*
Radiation interactions	*Not activated*
Transport size bins	*5 dust bins, log-normal size distribution; effective radii of 0.73 µm, 1.4 µm, 2.4 µm, 4.5 µm, and 8 µm*
Data assimilation	*Currently not activated (assimilation of MODIS AOD and ground-based PM2.5 measurements possible)*
Model original coordinates	*Regular latitude-longitude grid*
Dust output parameters	
SCONC_DUST	*Total dust mass concentration at the first model layer above the topography.*
AOD550_DUST	*AOD is calculated per layer based on mass extinction coefficients for mass concentrations per mode, then summed to obtain total column AOD.*
Model output for WMO SDS-WAS	*File format: netCDF* *Grid: regular latitude-longitude* *Longitude: 450 grid points* *Latitude: 325 grid points* *Time: 72 time steps, 3-hourly vector starting at 00 UTC* *Variables: SCONC_DUST, OD550_DUST*
References	*Grell et al. (2005); LeGrand et al. (2019)*

7.1.20. MOCAGE

Model	*MOCAGE*
Institution	*METEO FRANCE*
Meteorological driver	*ARPEGE (METEO FRANCE NWP Model)*
Domain of simulation	*Global*
Meteorological initial fields	*ARPEGE*
Emission scheme	*Marticorena and Bergametti (1995)*
Time step	*Advection time step : 1h / Chemical time step : 15min*
Horizontal resolution	*1°*
Vertical resolution	*47 levels*
Height first layer	*~20m*
Radiation interactions	*N/A*
Transport size bins	*6 bins (2.0E-3, 0.01, 0.1, 1, 2.5, 10, 50 microns)*
Data assimilation	*Hourly 3D-VAR assimilating AOD 550nm from MODIS (on Terra/Aqua satellites) and VIIRS (on NPP and NOAA20 satellites) instruments*
Model original coordinates	*1° x 1° regular grid*
Dust output parameters	
SCONC_DUST	*Total dust mass concentration present in the first model layer*
AOD550_DUST	*Dust AOD at 550nm*
Model output for WMO SDS-WAS	*File format: NetCDF* *Grid: Regular Lat-Lon Region : Lon : -25°E-65°E ; Lat : 0°N:65°NResolution 1°* *Time: Instantaneous values every 3hours ; validity time up to +72h, one production per day : basetime D-day 00hutc* *Variables: SCONC_DUST, OD550_DUST*
References	*Martet et al (2009), Sic et al (2015), Guth et al (2016), Sic et al (2016), El Amraoui et al (2022)*

7.1.21. Appendix B: AERONET stations used in the evaluation

Site name	Longitude	Latitude	Country	Region
Avignon	4.88°E	43.93°N	France	**Mediterranean**
Banizoumbou	2.66°E	13.54°N	Niger	**Sahel/Sahara**
Barcelona	2.12°E	41.39°N	Spain	**Mediterranean**
Cabo_da_Roca	9.50°W	38.78°N	Portugal	**Mediterranean**
Caceres	6.34°W	39.48°N	Spain	**Mediterranean**
Cairo_EMA_2	31.29°E	30.08°N	Egypt	**Mediterranean**
Capo_Verde	22.93°W	16.73°N	Capo Verde	**Sahel/Sahara**
CUT-TEPAK	33.04°E	34.67°N	Cyprus	**Mediterranean**
Dakar	16.96°W	14.39°N	Sénégal	**Sahel/Sahara**
Eilat	34.92°E	29.50°N	Israel	**Mediterranean**
Ersa	9.36°E	43.00°N	France	**Mediterranean**
ETNA	15.02°E	37.61°N	Italy	**Mediterranean**
Evora	7.91°W	38.57°N	Portugal	**Mediterranean**
FORTH_CRETE	25.28°E	35.33°N	Greece	**Mediterranean**
Granada	3.60°W	37.16°N	Spain	**Mediterranean**
IASBS	48.51°E	36.70°N	Iran	**Middle East**
IER_Cinzana	5.93°W	13.28°N	Mali	**Sahel/Sahara**
Ilorin	4.34 °E	8.32°N	Nigeria	**Sahel/Sahara**
IMAA_Potenza	15.72°E	40.60°N	Italy	**Mediterranean**
IMS-METU-ERDEMLI	34.26°E	36.56°N	Turkey	**Mediterranean**
KAUST_Campus	39.10 °E	22.30 °N	Saudi Arabia	**Middle East**
Kuwait University	47.97 °E	29.33 °N	Kuwait	**Middle East**
Lampedusa	12.63°E	35.52°N	Italy	**Mediterranean**
Lecce_University	18.11°E	40.33°N	Italy	**Mediterranean**
Oujda	1.90°W	34.65°N	Morocco	**Mediterranean**
Ouarzazate	6.91°W	30.93°N	Morocco	**Sahel/Sahara**
Palma_de_Mallorca	2.62°E	39.55°N	Spain	**Mediterranean**
Porquerolles	6.16°E	43.00°N	France	**Mediterranean**
Rome_Tor_Vergata	12.65°E	41.84°N	Italy	**Mediterranean**
Saada	8.16°W	31.62°N	Morocco	**Sahel/Sahara**

Santa_Cruz_Tenerife	**16.25°W**	**28.47°N**	**Spain**	**Sahel/Sahara**